# Inside the matrix

## Exploring the variability of mudstone and grog in archaeological ceramics using microanalytical methods

Pincé, Possum; Abdali, Negar; Braekmans, Dennis

**DOI**
10.1016/j.jas.2025.106419

**Publication date**
2025

**Document Version**
Final published version

**Published in**
Journal of Archaeological Science

Journal of Archaeological Science 184 (2025) 106419

Contents lists available at ScienceDirect

Journal of Archaeological Science

journal homepage: www.elsevier.com/locate/jas

# Inside the matrix: Exploring the variability of mudstone and grog in archaeological ceramics using microanalytical methods

Possum Pincé [a,b,*], Negar Abdali [c], Dennis Braekmans [d,e,f]

[a] Department of Archaeology, Ghent University, Sint-Pietersnieuwstraat 35, 9000, Ghent, Belgium
[b] OD Earth and History of Life, Royal Belgian Institute of Natural Sciences, Vautierstraat 29, 1000, Brussels, Belgium
[c] Prehistory and Near Eastern Archaeology, University of Heidelberg, Sandgasse 7, 69117, Heidelberg, Germany
[d] Laboratory for Material Culture Studies, Department of Archaeological Sciences, Faculty of Archaeology, Leiden University, Einsteinweg 2, 2333 CC, Leiden, the Netherlands
[e] Materials Science and Engineering, Faculty of Mechanical Engineering, TU Delft, Mekelweg 2, 2628 CD, Delft, the Netherlands
[f] Division of Geology, Department of Earth and Environmental Sciences, Celestijnenlaan 200E, 3001, Heverlee, Belgium

ARTICLE INFO

*Keywords:*
Archaeological ceramics
Mudstone
Grog
Ceramic petrography
SEM-EDS
Kur River Basin (Iran)

ABSTRACT

The differentiation between various fine-grained and clay-rich materials, also described as argillaceous inclusions, specifically mudstones and grog, presents considerable challenges in the analysis of archaeological ceramics. These difficulties arise from overlapping characteristics and the mineral uniformity of raw materials in certain environments. This study addresses these challenges by developing an interpretative framework to identify robust characteristic features to distinguish between mudstone and grog as well as recurring pitfalls. To this end, we constructed an experimental reference set comprising 26 testbars, which are analyzed using thin section petrography and SEM-EDS to examine the features of mudstone, grog and clays. The materials derive from the Kur River Basin in Southwest Iran, as this is an area with evidenced presence and use of extensive argillaceous inclusions through time. Additionally, we studied thin sections from a variable selection of archaeological ceramics (n = 11) with argillaceous inclusions from the same region that date from the Banesh to Late Bronze Age periods (ca. 3500 to 900 BCE) for comparison. The aim of this research was threefold: (1) assess optical identifiable characteristics of the argillaceous materials, (2) determine the compositional variability in the mudstones and grog fragments in this region and (3) document and test the potential of mudstone analysis for characterization and provenance purposes. Our findings indicate that distinguishing features are influenced by the granularity of the grog and sintering process. Notably, characteristics associated with mudstone inclusions comprise a compact, fine-grained texture, homogeneity with few to no constituents, solid or polygonal cracking, higher roundness, variability in particle sizes, and a pronounced likelihood of birefringence at lower firing temperatures where sintering has not yet occurred. The differentiation challenges intensify once sintering develops at higher firing temperatures, particularly when fine grog is present. In such cases, the angularity of the inclusions emerges as the primary criterion. SEM-EDS analysis further corroborated the established criteria, demonstrating a consistent chemical difference between grog and mudstone, aside from one overlapping type. Moreover, it supports a typological approach for determining these characteristics in thin section petrography and highlights a potential for provenance determinations of mudstone within a regional framework. Finally, analysis of the argillaceous inclusions in the archaeological ceramics suggests that no grog was used in these ceramics and that an intra-basin variability of mudstone was present that allows for higher resolution provenance studies.

## 1. Introduction

Petrographic analysis of ceramic thin sections has been a major established technique in the past decades to characterize and identify ancient ceramics all over the world. It enables a tracing of function and provenance on ceramics, as well as technological developments such as temper selection and fire temperature assessment. A known problem herein is the determination and classification of argillaceous inclusions.

* Corresponding author. Department of Archaeology, Ghent University, Sint-Pietersnieuwstraat 35, 9000, Ghent, Belgium.
*E-mail address:* Possum.Pince@UGent.be (P. Pincé).

https://doi.org/10.1016/j.jas.2025.106419
Received 16 May 2025; Received in revised form 24 October 2025; Accepted 26 October 2025
Available online 14 November 2025

More specifically, the differentiation between grog, (natural) clay pellets, clay temper and argillaceous rock fragments (ARF) such as mudstones and siltstones. Given their shared characteristics, it is often exceedingly difficult to firmly define grog particles, or reused/recycled ceramics, opposed to natural inclusions such as mudstones and clay pellets, certainly in environments where mineral resources are rather homogeneous. While a correct differentiation of these argillaceous inclusions is imperative for technological and provenance studies of ceramics, only a few reference studies discussing criteria for distinguishing various types of argillaceous inclusions with thin section petrography are present (Cuomo di Caprio and Vaughan, 1993; Eramo, 2020; Holmqvist, 2021; Quinn, 2013; Whitbread, 1986). However, the existing criteria need to be expanded for new situations as the ongoing challenges in differentiation often remain.

Argillaceous rock fragments are composed of lithified clay and silt, commonly referred to as mudstones and siltstones. They can be naturally present or added as temper (Adams et al., 2015; Makarona et al., 2016; Potter et al., 2005; Whitbread, 1986). Grog, on the other hand, is a fragment of crushed pottery that has been used as temper (Eramo, 2020). Although grog is often characterized by its angular and heterogeneous nature (Eramo, 2020; Quinn, 2013), the particular distinction and delineation of grog particles can be highly complicated in different locations, as they come in many forms and sizes. In this paper, we focus on differentiating ARF, specifically mudstone, from grog, as this distinction remains the most challenging based on existing diagnostic criteria. Upon firing, the compact and fine-grained texture of mudstone can develop a range of characteristics that overlap with those of various grog types (Reedy, 2008). In contrast, distinguishing natural, Fe-rich clay pellets from ARFs or grog is generally more straightforward using existing criteria (Holmqvist et al., 2018; Quinn, 2013; Whitbread, 1986). This is primarily due to the pellets' unfired nature, frequent close textural resemblance to the surrounding clay matrix, generally more constant grain size and non-angular form (Holmqvist, 2021).

Temper practices can be governed by cultural, geological and functional factors, and provide valuable insights into human-landscape relations in association with technological knowledge and potter's choices (Rice, 1987; Rye, 1981). A clear advantage of grog, compared to other temper materials, is its ready availability at any production site, as it can be sourced directly from pottery waste (Öhlinger et al., 2023). Grog temper also strengthens the material while simultaneously lowering stress caused by expansion and shrinkage during the firing process itself. This is primarily because grog, having undergone thermal transformation, exhibits minimal shrinkage and has a thermal expansion behavior more compatible with that of the surrounding clay (Eramo, 2020; Wang et al., 2023). In contrast, natural inclusions such as rock fragments can generate internal stress, increasing the risk of microcracks due to their differing thermal expansion. Fine-grained sedimentary rocks such as mudstones can reduce the clays' plasticity and enhance the density and compactness of the ceramics (Eramo, 2020; Matson, 1972; Rye, 1981; Santacreu Albero, 2014; Whitbread, 1995), potentially improving strength depending on their composition (Whitbread, 1995). Their relatively predictable performance makes them a practical and reliable temper choice, particularly in regions where mudstones are present. Besides the accessibility of these materials in the surrounding landscape, temper selection thus also depends on functional requirements, technological knowledge, and the properties of the clay itself, such as plasticity and shrinkage behavior (Cuomo di Caprio and Vaughan, 1993; Rice, 1987).

Cultural traditions and the scale of production further shape these practices. Household potters often use locally available materials and flexible recipes, whereas specialized or centralized production contexts tend to favor standardized temper compositions for consistency and quality control (Arnold, 1985; Costin, 1991; Santacreu Albero, 2014). Together, these factors influence how potters prepare their clay and fire their vessels. Moreover, ceramic vessels can be an integral part of social display and/or belief systems across generations (Gosselain, 1999; Kreiter et al., 2017; Mason and Cooper, 1999). Continuing traditions and clear examples of the cultural addition of temper can also still be found in modern societies (Barley, 1994; Gosselain, 2008; Gosselain and Livingstone-Smith, 2005).

This study reflects and builds on the criteria and methodology to differentiate grog and mudstone in archaeological ceramics by using optical transmitted light microscopy (thin section petrography) and variable pressure scanning electron microscopy coupled with an energy dispersive spectrometer (SEM-EDS). Experimental work and reference data have been collected in which the properties of different types of grog and mudstones in fired clays at various temperatures were compared in order to obtain a basis for solid discrimination criteria. For this, we used grog types and archaeological ceramics from Southwest Iran, more specifically from the Kur River Basin in the Zagros mountain range, where mudstone outcrops are common (Pincé et al., 2018, 2019). This region is of particular interest and can serve as an example since a varied and complex range of argillaceous inclusions are abundantly present in ceramic productions from the Banesh to the late Bronze Age period, spanning a time frame from ca. 3500 to 900 BCE. This also enables an extensive comparative for the characterization and variation of ceramics and mudstones in Southwest Iran and beyond. More specifically, we will determine the petrographic and chemical characteristics and variability in the mudstones, clay pellets and grog fragments in this region, develop an interpretative reference framework for the discrimination and provenancing of mudstone, and define its current limitations. While this study is grounded in the Kur River Basin, the overarching aim is methodological, namely to provide a revised reference framework and criteria that are transferable to other regions where the distinction between mudstone and grog presents similar challenges.

## 2. Materials and methods

### 2.1. Experimental material and archaeological sample selection

#### 2.1.1. Experimental data

The availability of comparable reference data is crucial to define this complex type of material. Therefore, both an experimental approach as well as an archaeological ceramic collection have been studied. For the reference database of grog, mudstone and raw clay materials, an experimental batch of 26 testbars was made (Table 1). The aim is to evaluate the distinguishing features of different types of argillaceous inclusions based on the experimental research and compared to existing reference frameworks from other studies (Cuomo di Caprio and Vaughan, 1993; Holmqvist, 2021; Quinn, 2022; Whitbread, 1986).

First, unfired reference blocks of three types of Iranian mudstones were produced to determine the characteristics and variability of the mudstones. The mudstone types used for these experimental testbars derive from the Zagros mountain range in Southwest Iran, namely from Ardakan and Jahrom in the Fars province, and one from the area around Isfahan (Isfahan province). They were chosen to capture the natural variability of mudstones relevant to the studied ceramics, which derive from the Kur River Basin in the Fars province. The location of the sampled mudstones and of the Kur River Basin are shown in Fig. 1. For the Isfahan area mudstone, only the general area could be determined.

These three types of mudstone were analyzed as is but were also added as temper to a commercially available clay (Sibelco K143) (technical data sheet: tinyurl.com/SibelcoK143). This standardized, homogeneous commercial clay was selected to ensure a consistent background matrix for comparison across the different inclusion types. The testbars for each mudstone temper were made in triplicate and fired under controlled conditions in a Nabertherm P300 kiln. The firing sequence involved a heating rate of 100 °C/hour, with maximum temperatures at 600 °C, 800 °C and 950 °C, followed by a soaking time of 1 h and a cooling rate of 50 °C/h. The firing was conducted in an oxidizing atmosphere to evaluate the characteristic features of mudstone temper at differing firing temperatures. These conditions reflect the estimated

**Table 1**
List of the experimental testbars (ITB) with additional information (IM = Iranian mudstone, ST = straw temper, GT = grit temper). *Ceramic samples from the Penn Museum (USA) with associated sample codes.

| ITB nr. | Material | Type temper | Temp. (°C) | Grain Size Mudstone |
|---|---|---|---|---|
| Testbar 1 | clay only (Sibelco K143) | – | 600 | – |
| Testbar 2 | 20 wt% Mudstone | Ardakan mudstone | 600 | 250–750 μm (max 1000 μm) |
| Testbar 3 | 20 wt% Mudstone | Jahrom mudstone | 600 | 250–750 μm (max 1000 μm) |
| Testbar 4 | 20 wt% Mudstone | Isfahan area mudstone | 600 | 250–750 μm (max 1000 μm) |
| Testbar 5 | clay only | – | 800 | – |
| Testbar 6 | 20 wt% Mudstone | Ardakan mudstone | 800 | 250–750 μm (max 1000 μm) |
| Testbar 7 | 20 wt% Mudstone | Jahrom mudstone | 800 | 250–750 μm (max 1000 μm) |
| Testbar 8 | 20 wt% Mudstone | Isfahan area mudstone | 800 | 250–750 μm (max 1000 μm) |
| Testbar 9 | clay only | – | 950 | – |
| Testbar 10 | 20 wt% Mudstone | Ardakan mudstone | 950 | 250–750 μm (max 1000 μm) |
| Testbar 11 | 20 wt% Mudstone | Jahrom mudstone | 950 | 250–750 μm (max 1000 μm) |
| Testbar 12 | 20 wt% Mudstone | Isfahan area mudstone | 950 | 250–750 μm (max 1000 μm) |
| Testbar 13a | 20 wt% Grog ST | Ceramic 85_61_76* | 600 | 250–750 μm (max 1000 μm) |
| Testbar 13b | 20 wt% Grog ST | Ceramic 85_61_76* | 800 | 250–750 μm (max 1000 μm) |
| Testbar 13c | 20 wt% Grog ST | Ceramic 85_61_76* | 950 | 250–750 μm (max 1000 μm) |
| Testbar 14a | 20 wt% Grog GT | Ceramic 85_11_235* | 600 | 250–750 μm (max 1000 μm) |
| Testbar 14b | 20 wt% Grog GT | Ceramic 85_11_235* | 800 | 250–750 μm (max 1000 μm) |
| Testbar 14c | 20 wt% Grog GT | Ceramic 85_11_235* | 950 | 250–750 μm (max 1000 μm) |
| Testbar 15 | Local alluvial clay (near Tall-i Siyah) | – | 800 | Not sieved |
| Testbar 16 | Local colluvial clay (near Tall-i Kureh) | – | 800 | Not sieved |
| Testbar 17 | 50 wt% Mudstone | Ardakan mudstone | 600 | 500–3000 μm |
| Testbar 18 | 50 wt% Mudstone | Ardakan mudstone | 800 | 500–3000 μm |
| Tesbar 19 | 50 wt% Mudstone | Ardakan mudstone | 950 | 500–3000 μm |
| IM-ARD | Ardakan mudstone | – | Unfired | – |
| IM-JAH | Jahrom mudstone | – | Unfired | – |
| IM-ISF | Isfahan area mudstone | – | Unfired | – |

firing range of the studied ceramic wares, as indicated by previous research (Blackman, 1981; Emami et al., 2021; Pincé, 2018; Pincé et al., 2019). The selected firing temperatures are representative of typical ranges for archaeological ceramics and capture three key stages in thermal transformation, namely before, during and after major mineral changes (Daszkiewicz and Maritan, 2016; Emami et al., 2021; Thér, 2014). Added mudstone inclusions at 20 wt% (percent by weight) were selected between 250 μm and 750 μm with a maximum size of 1000 μm to replicate a grain size similar to what is expected in common archaeological ceramics. The fine Ardakan mudstone testbar samples were made in two sequences, one following the standard procedure, and one with enhanced inclusion sizes (500 μm–3000 μm) and up to 50 wt% inclusions, as it was noted that during production and mixing this particular mudstone, it was prone to partial disaggregation into the clay matrix, likely due to contact with water when plasticizing the clay. This made them more difficult to identify with certainty in the standard procedure and may also explain their present-day popularity as a hair product in Iran (tinyurl.com/ArdakanMudstone1, May 8, 2025). However, the increase in the grain size of these inclusions could affect the reaction rates of the microstructure of the groundmass (Daszkiewicz and Maritan, 2016; Heimann and Maggetti, 2014). Macroscopically, the Ardakan mudstone shows a homogeneous and fine-grained texture similar to that of the Isfahan area mudstone, whereas the Jahrom mudstone is more heterogeneous with calcareous features (Fig. 2).

Additionally, testbars of two types of grog were made following our standard sieving and firing procedure. The selected grog samples derive from different archaeological ceramic wares, namely straw-tempered and grit-tempered wares dating to the Banesh period (ca. 3400 - 2900 BCE) in the Kur River Basin, which corresponds with the Proto-Elamite period in Iran. The samples originate from the archaeological site of Tall-i Malyan, also called Anshan (Fars province, SW Iran), which was one of the main Elamite cities (Alden et al., 1982; Alden and Petrie, 2015). These samples represent the two main types of ceramic inclusions that occur in ceramic wares in the study area from the Neolithic to the Late Bronze Age. Straw-tempered ware was typical for the Kur River Basin in the first pottery production during the Neolithic (ca. 6400-5000 BCE) and returned in the Banesh period, around 3400 BCE (Alden et al., 2004). The Banesh straw-tempered ware did not reach firing temperatures exceeding 725 °C (Blackman, 1981). Grit-tempered ware (crushed mineral rock or grog as inclusions), on the other hand, was introduced as a new ceramic type in the basin along the straw-tempered ware from the Banesh period onwards, and is considered a high-fired ware with firing temperatures of at least 900–950 °C in the Banesh period (Blackman, 1981, 1988). Straw and grit temper remained in use during the following Kaftari period (2200-1600 BCE) and grit-tempered ceramics occurred until the subsequent Late Bronze Age (1600/1300-900 BCE) in this region (Alden, 1979; Pincé, 2018; Sumner, 1991, 2003). For the straw-tempered reference grog, a Banesh sherd of Tall-Malyan (unit ABC) was partially used (Code No. 85-61-76). For the grit temper, part of a Banesh sherd from Malyan TUV was selected (Code No. 85-11-235). The sample codes refer to the collection codes of Penn Museum (USA) where the ceramic samples are stored.

To determine the variability of the clays in the study region and the possible presence and characteristics of natural argillaceous inclusions, testbars were made of an alluvial clay sample near archaeological site Tall-i Siyah (coordinates WGS84: N 30°03.111′, E 52°36.301′) and a colluvial sample near the site of Tall-i Kureh (N 30°08.003′, E 52°27.488’) in the Kur river basin in Iran. The testbars were fired at 800 °C (Alden, 2013; Pincé, 2018; Sumner, 1972). The locations of these samples are shown in Fig. 1.

### 2.1.2. *Archaeological ceramics*

Besides the use of archaeological straw-tempered and grit-tempered Banesh ceramics from the Kur River Basin in the reference dataset, 11 archaeological ceramics with abundant argillaceous inclusions (8–40 %) were selected. These samples are representative of local ceramic wares dating from the end of the fourth millennium BCE to ca. 900 BCE, and include Banesh, Kaftari, Middle Elamite, Shogha and Taimuran wares (Pincé, 2018; Pincé et al., 2019). The latter three wares correspond to the Late Bronze Age in the Kur River Basin, contemporaneous with the Transitional and Middle Elamite phases in Khuzistan (Carter and Stolper, 1984). The selection was based on an extensive petrographic and X-ray fluorescence (XRF) analysis of 356 ceramics from the Neolithic to Late Bronze Age period in the Kur River Basin, undertaken to better understand the ceramic technology and provenance in a region where these aspects had previously been little investigated (Pincé, 2018; Pincé et al., 2018, 2019).

## 2.2. *Methodology*

The dataset consisting of both experimental testbars, natural clays and ancient ceramics is subsequently studied using micro-analytical techniques that are commonly applied in ceramic research, i.e., optical microscopy and SEM-EDS. This approach is aimed at determining the

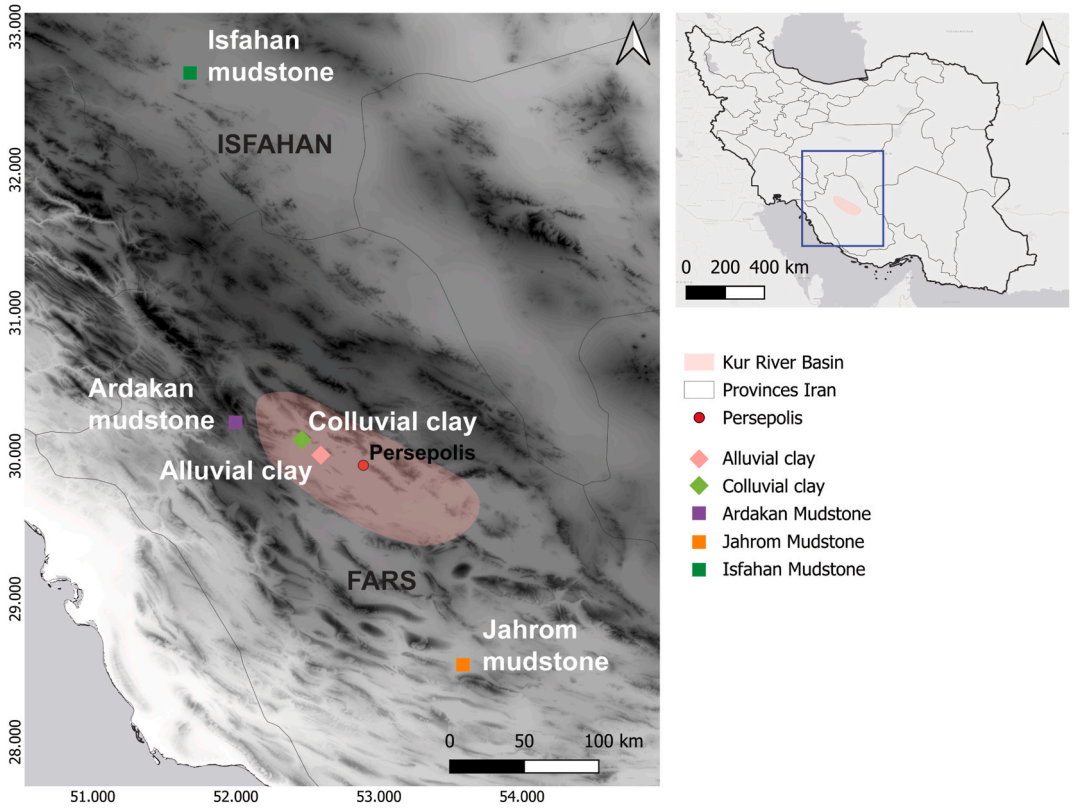


**Fig. 1.** Location of the reference mudstones and reference clays, and the study area associated with the archaeological ceramics.

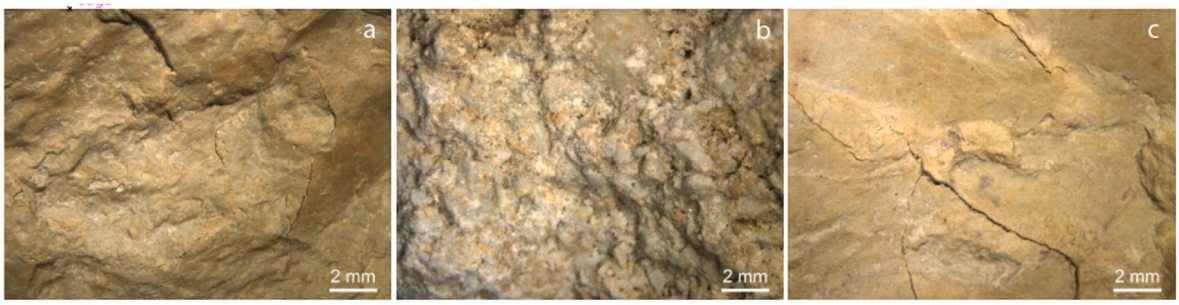


**Fig. 2.** Stereomicroscopic images of natural mudstone from Ardakan (a), Jahrom (b) and the Isfahan area (c) that illustrate the encountered regional variation.

characteristics, variability and assessing the differentiation potential of mudstone and grog inclusions. Additionally, this information can be used to explore their potential for provenancing and identifying specific technological temper and firing procedures.

### 2.2.1. *Thin section petrography*

To study the petrographic characteristic features of the reference grog and mudstones in comparison to those in archaeological ceramics, thin sections of 26 experimental testbars and 11 archaeological ceramics have been studied with optical light microscopy (Quinn, 2022). Thin section analysis was performed using a NIKON Eclipse LV100N POL microscope at Ghent University (Belgium), and photomicrographs were systematically taken at 40× magnification. Petrographic descriptions of the archaeological ceramics have already been performed and described in Pincé (2018) and Pincé et al. (2019). Therefore, in this study, we focus solely on a detailed description of the characteristics of the argillaceous inclusions, building further on characterization procedures operationalized by i.a. Cuomo di Caprio and Vaughan (1993), Holmqvist (2021), Quinn (2022) and Whitbread (1986). The photomicrographs presented in the figures are also included in full resolution in the Supplementary Material, along with a descriptive list detailing general information about each photomicrograph.

### 2.2.2. *SEM-EDS*

In order to compare the composition of the clay materials, mudstones, grog and clay pellets in the archaeological samples, a SEM-EDS analysis was performed on a selection of experimental testbars and ceramics as in thin section petrography. This technique has the advantage of targeting discrete inclusions on a microchemical scale to contribute chemical compositional information of specific mudstone, grog, clay and clay pellet inclusions (Tite et al., 1982).

Chemical analysis of the studied materials was conducted with two variable pressure scanning electron microscopes coupled with energy-dispersive X-ray spectroscopy, a Hitachi SU3500 at Cranfield University (Defence Academy of the United Kingdom, United Kingdom) and a Tescan Mira 3 at Ghent University (Belgium). For the SEM-EDS analysis, polished archaeological thin sections were used as well as experimental material embedded in epoxy resin and polished prior to analysis. The

instruments were operated at 20 kV, with a measuring livetime of 120 s at a working distance of 10 mm. The selection of analysis locations was based on identifying a representative set of non-plastic argillaceous inclusions, avoiding other large inclusions and correlating directly to inclusions described in the petrographic analysis. A total of 194 measurements have been performed, both point and area measurements to document variability. Analytical accuracy and precision were checked through routine analysis of external standards (see also Norris et al., 2022), applying a standardless ZAF quantification (Reed, 2005).

## 3. Results

### 3.1. Petrography

The petrographic analysis of the fired reference mudstones and grogs was conducted based on the classification criteria initially set forth by Whitbread (1986), and Cuomo di Caprio and Vaughan (1993). However, it became evident that the application of these criteria proved only partially applicable to the mudstone-grog-clay problem examined here; this issue is addressed further in Section 4.1. As a result, we identified and described the specific characteristics that were effective and under which circumstances, as well as additional distinguishing features to successfully differentiate mudstones from grogs.

#### 3.1.1. Unfired reference mudstones

Petrographic analysis of the experimental testbars of the reference mudstones can be characterized as fine-grained, relatively homogeneous mudstones with Fe-rich concentrations that are visible as dark red to reddish brown areas. The mudstone from Jahrom has the most heterogeneous fabric, including more carbonate-rich components in an overall fractured texture. The Isfahan area mudstone further shows a Ca-rich matrix and has Fe-rich concentrations in an otherwise fine-grained matrix (Fig. 3). Planar voids and striations are related to the preparation of thin sections, which is challenging due to the softness of the mudstones.

#### 3.1.2. Fired reference mudstones in clay matrix

The fine-grained and relatively homogeneous characteristics described in the reference mudstone thin sections persist throughout the crushing, incorporation as temper in clay and subsequent firing. In firing the testbars at 600 °C and 800 °C, no discernible alterations are observed in the characteristics of the mudstones. However, at 950 °C, a much lower optical activity can be identified, making the mudstones optically more isotropic. Additionally, shrinkage voids around the inclusions often appear in combination with occasionally few cracks in the microstructure.

Furthermore, the mudstone from the Isfahan area shows a high calcium content, which likely reflects the presence of calcium carbonate that already decomposes below the temperature of 950 °C. This particular type of mudstone exhibits a more angular contour than the other mudstone types, probably related to a higher hardness of the calcareous mudstone. The shapes of Isfahan area mudstone temper vary from conchoidal to prolate, while those from the Ardakan and Jahrom mudstones range from prolate to equant within the same type. The Fe-rich Ardakan mudstone shows many various shapes at a firing temperature of 950 °C, while the calcareous Isfahan area mudstone is more fragmented, likely resulting from internal stress generated during calcite decomposition (Cultrone et al., 2001; Fabbri et al., 2014). The colors in PPL and XP are mudstone-type specific and are darker at a firing temperature of 950 °C due to the sintering process. The Jahrom mudstone has clear boundaries and is less compact than the other mudstone types, which leads to a more neutral optical density (Whitbread, 1986). The Ardakan and Isfahan area mudstones have sharp boundaries and a high optical density that makes them appear more opaque than their matrix. The high Fe-content of Ardakan mudstone and high Ca-content of Isfahan area mudstone may have also contributed to that. Additionally, the Jahrom and Isfahan area mudstones are still birefringent when fired to 600 °C and 800 °C, while the more Fe-rich Ardakan mudstone shows minimal to no birefringence. At a temperature of 950 °C, all the mudstone types lose their birefringence (Fig. 4, Table 2).

#### 3.1.3. Fired reference grog in clay matrix

Grog in these testbars shows a generally more heterogeneous and less compact composition than the experimental mudstone temper. In contrast to the mudstone inclusions, small shrinkage voids are noticed around most grog fragments in the different testbars, regardless of the grog type or firing temperature, while for the tested mudstones, it is mainly linked to a higher firing temperature above 800 °C. The heterogeneity of the grog is related to mineral inclusions for ST and GT types, and in the GT grog, other argillaceous inclusions are also present. The angularity of the reference grog samples varies from subrounded to angular for the ST grog, while the GT grog is more angular. The shapes of ST grog range from equant to prolate, while the GT grog fragments are prolate or have a more fragmented and shattered look, as is visible in Fig. 5. No equant shapes are present in the current dataset. Also, no systematic alignment or stress fractures parallel to the greatest dimensions of the grog fragments are noted. The ST grog fragments have a neutral optical density and clear boundaries, while for the GT grog, a variable optical density and sharp boundaries are visible. The optical density for GT grog in clay fired at 600 °C and 800 °C was high, but at 950 °C it becomes neutral due to the higher firing temperature. The ST grog at 950 °C is the hardest to differentiate from mudstone (Fig. 5, Table 2). The most important characteristic feature here is a clear heterogeneity compared to other inclusions inside the grog, which is not present to that extent in any of the mudstones.

Although grog and mudstone were both added at 20 wt%, the apparent frequency of inclusions differs because the lower density and higher porosity of grog result in a larger volumetric proportion within the clay matrix compared to the denser mudstone.

#### 3.1.4. Fired natural Iranian clays

Two different clays from the Kur River Basin in Iran were fired at 800 °C to determine the natural inclusions and variability inside these clays (Fig. 6). The first clay type is derived from an alluvial context near

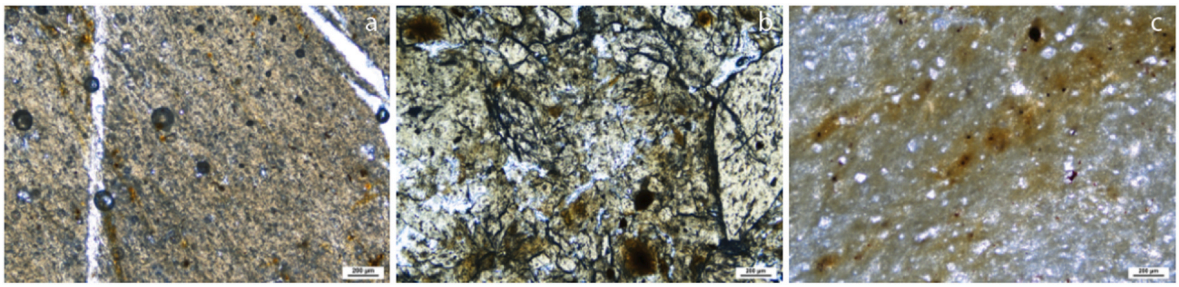


**Fig. 3.** Thin section photomicrographs in PPL of natural mudstone from Ardakan (a), Jahrom (b) and the Isfahan area (c).

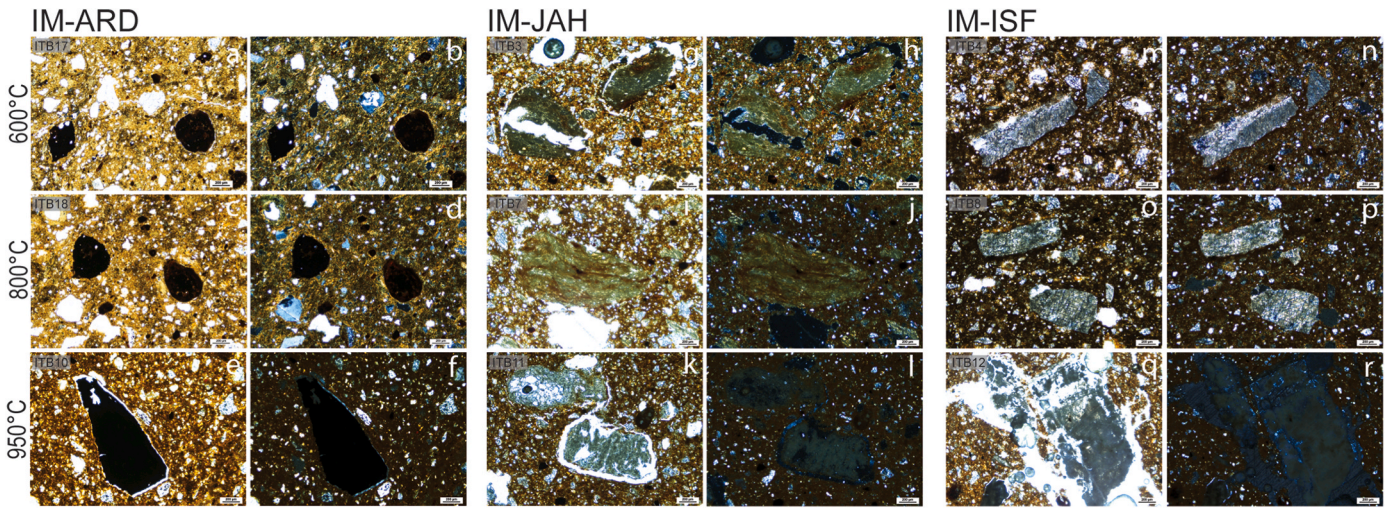


**Fig. 4.** Thin section photomicrographs (a–r) of the reference mudstones in clay, fired at different temperatures, in PPL (left) and XP (right).

Tall-i Siyah and is a relatively fine-grained clay without a visible presence of mudstone. However, small iron concretions and especially irregular shaped iron-rich nodules are present. The second selected clay type is a colluvial clay that is more enriched in calcareous materials.

### 3.1.5. *Argillaceous inclusions in archaeological ceramics*

The diagnostic petrographic features that are characteristic for mudstone and grog observed in our experimental dataset above are used to identify the type of 'unknown' argillaceous inclusions in archaeological ceramics. The descriptive approach consists of evaluating especially the homogeneity, alignment of the internal microstructure (orientation of constituents and voids), character of the microstructure (cracking and stress fractures), roundness, shrinkage voids, birefringence and size range. Interestingly, no grog can be determined in these ceramics, suggesting that only mudstone temper was used in the grit-tempered Banesh, Kaftari, Shogha, Taimuran and Middle Elamite pottery. This supports the extensive petrographic characterization of these ceramic types in Pincé et al. (2019) and Pincé (2018). However, this is inconsistent with observations in a previous study that suggests the use of grog for Kaftari and Shogha pottery (Emami et al., 2021).

Additionally, a high variability of mudstone types are identified in the archaeological ceramics. This not only encompasses revised criteria for mudstone classification but also incorporates additional parameters such as color, optical density, degree of sintering, Fe-content, boundary sharpness and shape. These criteria are systematically indicative of specific mudstone types and may also reflect particular technological aspects, including firing temperature, clay matrix composition, and preparation processes that affect the outlook of the mudstones. As a result, we categorize the mudstones into eight distinct petrographic groups or types. Besides these mudstones, three types of clay pellets are identified, but no grog fragments (Fig. 7, Supplementary Table A).

## 3.2. *SEM-EDS*

A total of 194 SEM-EDS measurements were performed on the reference testbars and archaeological dataset, using both area and average values of the point analyses, unless indicated otherwise (Supplementary Table B). The results are expressed as oxide weight percentages and normalized to 100 %. The SEM-EDS analysis of the unfired reference mudstones shows clear differences in chemical composition. Ardakan mudstone has a high Fe-Ti, high K, while Jahrom is a high Mg mudstone. Both of these mudstones provide, repeatedly, consistent chemical results. The Isfahan mudstone is, however, much more heterogeneous and variable in its chemical composition. This type of mudstone is characterized by a high to extremely high Ca concentration (in a range of 40–80 wt%) as well as a systematically low $SiO_2$ and $Al_2O_3$. The chemical composition of the reference fired colluvial and alluvial clay of the Kur River Basin, has a lower percentage of CaO and slightly higher percentage of $Al_2O_3$ and $Fe_2O_3$ for the colluvial clay. The fired reference grog samples, on the other hand, seem to have a different elemental composition than the mudstones in the experimental testbars and archaeological ceramics, regardless of the type of grog used (ST or GT), the firing temperature and the clay matrix. The grit-tempered grog shows a higher $Fe_2O_3$ and high $Al_2O_3$, and lower MgO percentage in comparison to straw-tempered grog. Although CaO is quite variable, in general, lower CaO values are documented in the GT grog particles at approximately 14.5 wt% CaO in contrast to the ST grog samples averaged at approximately 17 wt%. The reference grog samples display a consistent, different composition from the mudstones in the reference testbars and archaeological ceramics. A main compositional difference between grog and the mudstones from local archaeological ceramics lies in the higher $Al_2O_3$ percentage for the archaeological mudstone groups, except for mudstone type 2.

A general discriminant analysis (DA) provided eight elements within the prediction model that are at significant levels $p < 0.05$, confirming the grouping proposed can be used in a valid way with these elements, namely Ca, K, Al, Na, Si, Ti, P and Mg (Supplementary Table C). Discriminant analysis (Fig. 8) confirms three different geochemical groups for the analyzed Iranian mudstones of Ardakan, Jahrom and Isfahan area. The mudstone groups identified in the archaeological ceramics through petrography show a different composition than the experimental Iranian mudstones. The exceptions are the mudstone types 2 and 8, which have a more similar composition to the natural mudstone of Jahrom and Ardakan, respectively, indicating a different provenance than the other archaeological mudstones. The other archaeological mudstone groups can be attributed to one larger geochemical group, but have different chemical compositions within this geochemical group. Furthermore, the analyzed archaeological mudstones and experimental grog from local archaeological ceramics occur in two clear separate compositional clusters, except for mudstone type 6. Both the GT and ST grog are, however, too variable in comparison to the other samples to differentiate into separate compositional groups. For this, petrography proves to be more suitable. The analyzed grog samples cluster together with the alluvial and colluvial fired clays at 600 °C and 800 °C. However, at 950 °C, the alluvial fired clay has a more heterogeneous and differing composition, which correlates with sintering processes visible in the petrography. SEM-EDS analysis of the Isfahan area mudstone fired at 800 °C and 950 °C reveals no significant changes in elemental composition. However, upon firing, the alluvial clay exhibits a slight compositional shift between 800 °C and 950 °C, likely resulting from

**Table 2**
Described petrographic characteristic features of the mudstone and grog present in the reference dataset. Terminology following Whitbread (1986) and Cuomo di Caprio and Vaughan (1993).

| | MUDSTONE | | | | | | GROG | | | |
|---|---|---|---|---|---|---|---|---|---|---|
| | IM-JAH | IM-JAH | IM-ISF | IM-ISF | IM-ARD | IM-ARD | Straw temper | Straw temper | grog temper | grog temper |
| | 600&800°C | 950°C | 600&800°C | 950°C | 600&800°C | 950°C | 600&800°C | 950°C | 600&800°C | 950°C |
| **Homogeneity** | Homogeneous | Homogeneous | Homogeneous | Homogeneous | Homogeneous | Very Homogeneous | Heterogeneous | Heterogeneous | Heterogeneous | Heterogeneous |
| **Relative granularity** | Fine-grained | Fine-grained | Fine-grained with few large Cb frags. | Very fine-grained | Fine-grained | Very fine-grained | Medium-grained | Medium-grained | Medium-grained | Medium-grained |
| **Microcrystallinity** | Yes | No | No | No | No | No | Yes | No | No | No |
| **Aligned internal microstructure** | Yes | No | Yes | No | No | No | No | No | No | No |
| **Character of internal structure** | Very few voids | Polygonal cracking, regular voids | Polygonal cracking | Polygonal cracking | Very few and small voids | Polygonal cracking, very few and small voids | No clear stress fractures, few voids | No clear stress fractures, few voids | No clear stress fractures, few voids | No clear stress fractures, few voids |
| **Roundness** | Rounded | Rounded to subangular | Angular to subrounded | Angular to subrounded | Rounded to subangular | Subrounded to angular | Subrounded to subangular | Subrounded to subangular | Subrounded to angular | Subrounded to angular |
| **Shrinkage voids** | Occasional | Occasional | Almost no voids | Occasional | No | Yes (clearly visible) | Yes (small margin) | Yes (small margin) | Yes (small margin) | Yes (clearly visible) |
| **Birefringent matrix in XP** | Yes | No | Yes | No | Low to no | No | Low | No | No | No |
| **Sintering** | No | Yes | No | Yes | No | Yes | No | Partially | Yes | Yes |
| **Optical density** | Neutral | Neutral | Low | High | High | High | Neutral | Neutral | High | High |
| **Boundary** | Clear | Clear | Clear to sharp | Clear to sharp | Clear to sharp | Sharp | Clear | Clear | Clear to sharp | Clear to sharp |
| **Shape** | Prolate to equant | Prolate to equant | Irregular to prolate | Irregular to prolate | Prolate to equant | Prolate to equant | Prolate to equant | Prolate to equant | Irregular to prolate | Irregular to prolate |
| **Colour PPL** | Grey | Grey | Grey | Dark Grey | Reddish Brown | Dark brown to black | Yellowish Brown | Brown Grey | Greyish Brown | Greyish to Reddish Brown |
| **Colour XP** | Grey | Grey | Grey | Dark grey | Dark reddish brown[a] | Dark brown to black | (Dark) yellowish brown | Dark brown grey | Dark (greyish) brown | Dark greyish to reddish brown |
| **Ferruginous** | No | No | No | No | Yes | Yes | No | No | Yes | Yes |

Cb frags. = carbonate fragments.
[a] similar to matrix but darker.

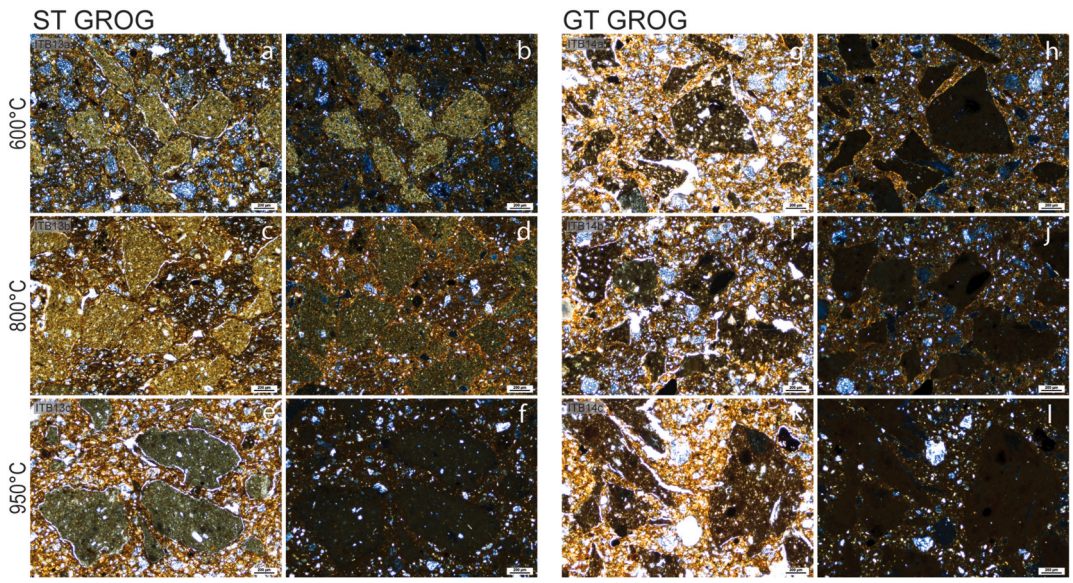


**Fig. 5.** Thin section photomicrographs (a–l) of the reference grog types in clay, fired at different temperatures, in PPL (left) and XP (right).

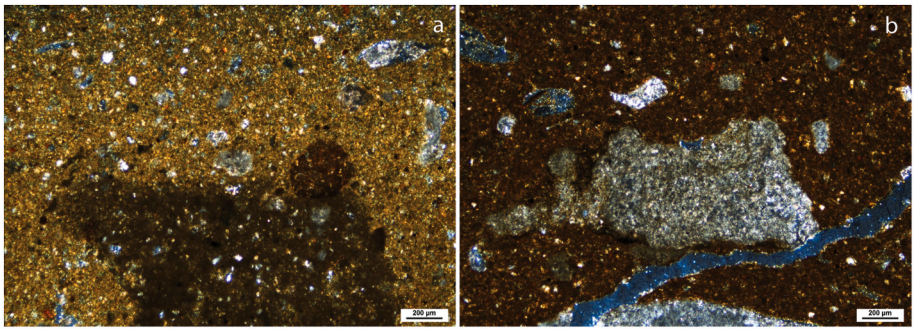


**Fig. 6.** Thin section photomicrographs (XP) of alluvial clay (a) and colluvial clay (b) fired at 800 °C.

increased densification associated with sintering and the formation of new silicate phases at these temperatures (for an overview of phase changes in earthenwares, see Gliozzo, 2020). Finally, the clay pellets show some variability but have a more similar geochemical composition to the mudstones than the grog.

## 4. Discussion

### *4.1. A re-evaluation of characteristic petrographic features of mudstone and grog*

This experimental comparative analysis investigates the characteristic features of mudstone and grog temper, and provides a comprehensive evaluation of the features identified in prior research (Cuomo di Caprio and Vaughan, 1993; Eramo, 2020; Quinn, 2013; Whitbread, 1986). A key feature identified in the experimental dataset is the homogeneity of the mudstones, characterized by a low amount of constituents and a fine-grained texture. According to Whitbread (1986) and Quinn (2013), ARFs may exhibit variations in texture, such as laminations or bedding, which can also be observed in the mudstone type from the Jahrom and Isfahan areas. In contrast, grog in the experimental dataset displays a more variable or higher degree of heterogeneity without evidence of bedding. Cuomo di Caprio and Vaughan (1993) suggest that the presence of an aligned internal microstructure, referring to a parallel orientation among constituents and voids, could be a useful criterion for distinguishing grog temper, but these are not observed in the grog samples of this dataset. As Cuomo di Caprio and Vaughan (1993) imply, this criterion is more likely useful for grog that was originally subjected to significant physical manipulation during preparation, such as wheel pressure or surface treatment.

A more generally applicable feature highlighted by Cuomo di Caprio and Vaughan (1993) is the character of the internal structure, where internal polygonal cracking is associated with ARFs, and cracks parallel to the greatest dimension characterize grog. In this dataset, internal polygonal cracking is observed in the mudstones, while grog samples display neither polygonal cracking nor stress fractures. Consequently, this study supports the use of internal polygonal cracking as a distinguishing feature for mudstones.

Another criterion for differentiating mudstones from grog is the roundness or angularity of inclusions (Eramo, 2020; Quinn, 2013; Whitbread, 1986). Whitbread (1986) states that mudstones can exhibit significant variability in this respect, ranging from angular to well-rounded, while grog is generally expected to be angular to subrounded. Our experimental data indicate a tendency for mudstones to be more rounded and abraded, occasionally reaching subangular forms. However, no angular mudstones are present in our samples. The roundness of the inclusions in the experimental grog vary between subrounded and angular, largely depending on the specific type of grog used. Notably, the straw-tempered grog exhibits a higher degree of roundness compared to the grit-tempered grog. Holmqvist (2021) suggests this variation might be attributed to a lower firing temperature of, in this case, the ST grog relative to the GT grog (Blackman, 1981). Another factor that may influence this phenomenon is the type of temper (e.g. straw or grit) used in the original ceramic, since this has an effect on

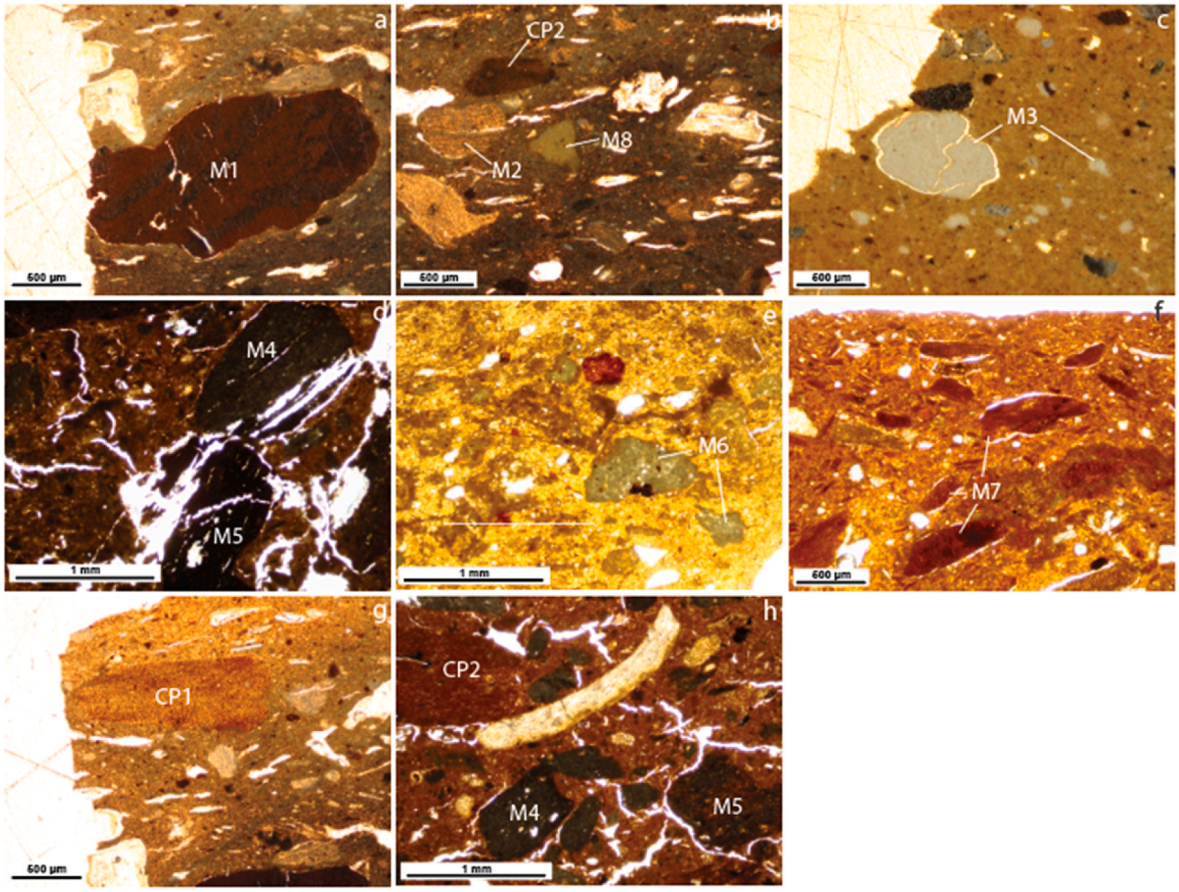


**Fig. 7.** Thin section photomicrographs (a–h) in PPL of the identified mudstone types and clay pellets in the archaeological ceramics from the Kur River Basin (Iran). No grog fragments were determined in these samples (M = mudstone, CP = clay pellet).

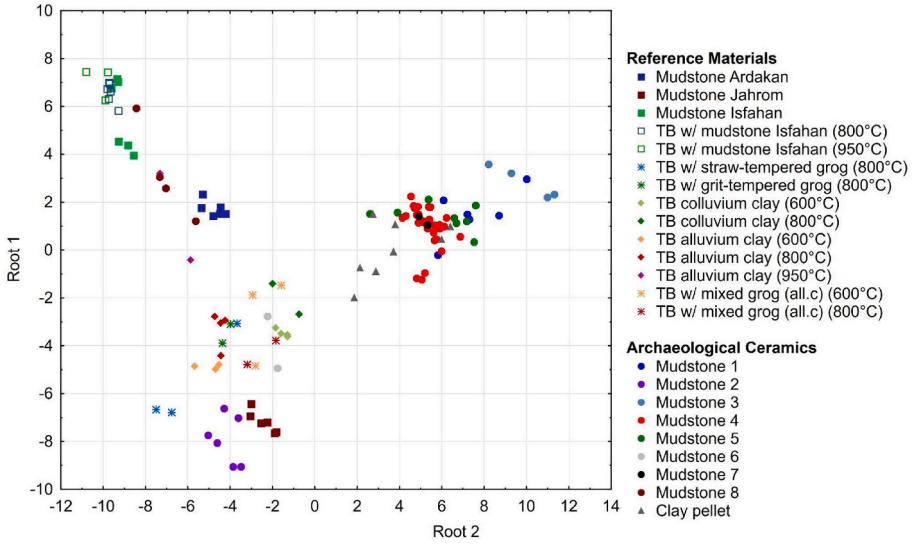


**Fig. 8.** Canonical score plot indicating group differentiation using canonical functions in discriminant analysis of archaeological ceramics, experimental testbars and geological reference samples related to mudstone, clay and grog enrichments.

the porosity of the material. Cuomo di Caprio and Vaughan (1993) further argue that angularity relates to the relative hardness of an inclusion and its composition. However, since grog is fired before being incorporated into the clay matrix and subsequently fired again, it typically exhibits greater hardness than natural mudstones. Mudstones primarily consist of relatively soft fine clay minerals, taking into account their composition and degree of lithification. Therefore, when significantly angular argillaceous inclusions are present, they are more likely to be grog. Additionally, smaller inclusions of mudstone tend to display more roundness than those of grog temper. It is also worth noting that, although Rye (1981) suggests that angularity may indicate the addition of temper, this perspective seems less likely for mudstones in particular,

as all experimental mudstones functioned as temper and predominantly exhibited rounded shapes (Rye, 1981).

A notable feature in our dataset is the presence of shrinkage voids surrounding mudstone inclusions at a high firing temperature (950 °C), when there is clear sintering, and rarely at lower firing temperatures, where the matrix remains unsintered. In contrast, grog temper consistently displays small shrinkage voids across all tested temperatures, both in sintered and unsintered matrices. Although Cuomo di Caprio and Vaughan (1993) state that shrinkage voids are not a useful criterion for distinguishing grog temper from ARFs, as their formation relates to compaction, composition and size, we argue that due to the differing compaction and composition between mudstones and grog, shrinkage voids can be a useful characteristic for distinction when considered in relation to the degree of sintering.

The exact temperature at which sintering begins depends on clay mineralogy, flux content, and firing conditions (Gliozzo, 2020; Maniatis and Tite, 1978; Thér, 2014; Tite, 1995). In our experimental series, clear evidence of sintering is observed at 950 °C, whereas samples fired below this temperature retain a microcrystalline clay matrix and inclusions without extensive sintering, consistent with lower firing regimes. Once extensive sintering occurs, roundness becomes the only reliable criterion for distinguishing mudstone from grog. As the grog and several mudstone types in this dataset are calcareous, the onset of sintering is likely to be initiated at lower firing temperatures than in non-calcareous clays (Fabbri et al., 2014; Gliozzo, 2020; Heimann and Maggetti, 2014). Nevertheless, in both calcareous and non-calcareous samples from the experimental and archaeological datasets, extensive sintering is observed between 800 °C and 950 °C.

Birefringence also proved to be a useful feature when considered in combination with other characteristics. Although it depends partly on the firing temperature and composition of the original ceramic used as grog, the grog samples generally show a higher tendency to lack birefringence and appear more opaque than mudstones at relatively low firing temperatures (here at 600 °C and 800 °C), given that the grog had already been fired prior. At higher temperatures (here from 950 °C onwards), mudstones also exhibit a loss of birefringence. It must be noted that when mudstones display a high iron content, they tend to appear more opaque, making this feature for these types of mudstones less useful for identification purposes. Furthermore, Whitbread's criterion of optical density to assess opacity and microcrystallinity relative to the matrix is found to be less suitable or indicative, as both mudstones and grog display neutral to high density and this criterion is relative to the surrounding matrix. This perspective is supported by Cuomo di Caprio and Vaughan (1993). It can, however, be a helpful criterion to differentiate between the majority of mudstone types as demonstrated in this study. Ultimately, this criterion is especially geared towards the identification of low iron-bearing potential mudstones.

A final feature that is observed to be useful to distinguish between mudstone and grog is their size range. While Cuomo di Caprio and Vaughan (1993) argue that all sizes can occur, both in grog and mudstones, and that if one size is present, this is primarily related to the technological process or skills of the potter of the inclusions; our experimental dataset shows that samples enriched in mudstone have a complete range of sizes, and grog tends to be more restricted in size range. This could be related to the fact that mudstones may partially disaggregate into the clay matrix when plasticizing the clay.

Other suggested characteristics, such as color, boundary sharpness and shape, seem to be more arbitrary and less effective in differentiating between mudstone and grog. The color is variable and depends on the composition of the mudstones and the firing conditions, as is also stated by Whitbread (1986). The boundaries vary between sharp and clear for both mudstone and grog, which seems to be more related to the composition of the inclusion, the similarity with the surrounding matrix, and the firing temperature. Regarding the shape, prolate shapes and conchoidal fractures are referenced as indicative of mudstones (Quinn, 2013; Whitbread, 1986). However, our dataset shows that prolate is not necessarily true for mudstone, and also equant shapes appear, making this feature less useful.

Finally, no mudstone fragments are present in the local alluvial and colluvial clay samples analyzed. In contrast, mudstone inclusions occur frequently and in significant quantities in the archaeological ceramics. This contrast suggests that mudstone was deliberately added as temper rather than occurring naturally in the local clays. Additionally, the presence of multiple mudstone types within the assemblage reflects the technological diversity, likely resulting from a complex interplay of practical (e.g. mixing different temper types, firing variability), as well as cultural, economic or environmental factors. Post-depositional alterations may also have contributed to this variability.

### 4.2. *Defining the chemistry of mudstone, grog and clay pellets in Iranian archaeological ceramics*

This section discusses the geochemical variability of mudstones, grog and natural clays in the Kur River Basin. The experimental testbars with Banesh straw- and grit-tempered grog and natural clays are chemically different from both archaeological and experimental mudstones. This is mainly related to the higher $Al_2O_3$ percentage than the local grog and clays, which indicates a generally higher clay content with an even grain size distribution for the mudstones than the grog in the region (Taylor and McLennan, 1985). When comparing the chemical composition between the experimental Iranian and archaeological mudstones, four distinct clusters of mudstone chemistry can be identified: (1) an Ardakan and Isfahan type group, including mudstone type 8, (2) a Jahrom, mudstone 2 group and (3) a Kur River Basin group consisting of mudstone types 1, 3, 4, 5 and 7 and a (4) clay- and grog group including mudstone type 6. Both mudstone 1 and 3 could be considered a subgroup as they diverge. The chemical variability between these mudstone types shows the potential for exploring the provenance of mudstones at a higher resolution.

Mudstone type 2, is more related to the Jahrom mudstone, indicating a different origin than the other archaeological mudstone types. If dealing with a marly or calcareous mudstone such as the Isfahan area mudstone, these can be easily distinguished based on the high Ca content opposed to regular ceramic matrix compositions (Lazar et al., 2015).

We further observe that mudstone types 1, 3, 4 and 5 were used in ceramics of different periods and ceramic styles, while the other mudstone types are associated with a specific ceramic sample or ware. Mudstone 1 is noted in Shogha ware from Tall-i Darwazeh and Banesh ware from Malyan TUV. Mudstone types 3, 4 and 5 occur in Banesh ware from Malyan TUV and Tall-i Kureh and buff Middle Elamite ware from Malyan. Mudstone type 4 is also present in Shogha ware from Tall-i Darwazeh. For the Kaftari red ware, a different type of mudstone is used as grit temper, namely mudstone type 6. Mudstone type 7 is only noted in Taimuran pottery from Tall-i Taimuran, and mudstone type 3 in Banesh pottery from Tall-i Malyan, section TUV. Different types of mudstones thus occur in the Banesh GT ware from the city of Tall-i Malyan. Only mudstone type 6 differs from all the other mudstone groups, and holds uniquely a range of CaO at ~25 wt%. The sample where this type is identified is the only Kaftari sample (85-61-43), potentially related to a different source of mudstone. In this case, thin section petrography is essential to enable a substantiated mudstone identification. Interestingly, mudstone type 2 is only identified in sample 85-61-66, and mudstone type 8 in sample 73-8-305, both of which relate to individual petrographic fabric groups (sedimentary-metamorphic and sedimentary-shale) (Pincé, 2018). Given that both of them are rare in the assemblage of the region, they might be considered imports to the Kur River Basin region.

A geochemical differentiation between the types of grog is less evident, which may suggest that although two different ceramic types are used as grog for the experimental dataset, the clay matrix to compose these original ceramics is similar and may point to a similar clay outcrop

and geological substrate. The alluvial and colluvial clay matrices also match the grog compositions, suggesting local clays were used to produce these ST and GT Banesh ceramics of Tall-i Malyan. The clay pellets' partial overlap in geochemical composition with most mudstone types is probably related to their shared homogeneity, higher clay content, and usually lower amount of inclusions than grog.

Important to note is that no clear grog is identified in the studied archaeological ceramics, which comprise Banesh GT and ST wares, Kaftari red ware, Shogha ware, Taimuran ware, and buff Middle Elamite ware. While it cannot be entirely ruled out that grog may have been used in other ceramic samples of these wares, caution is warranted in this regard, as the experimental work regarding the mudstones shows that these could easily be mistaken for grog without precise evaluation of their characteristic features and other archaeological information. More research on these ceramics using these criteria is needed to obtain a conclusive answer about the grog use itself, and the criteria should be systematically stated when a distinction in the type of argillaceous inclusions is made.

SEM-EDS analysis largely supports the revised characteristic features distinguishing mudstone and grog established through thin section petrography, by revealing significant differences in their elemental composition. While SEM-EDS is effective for detecting and comparing spatial and compositional variability between samples and inclusions, its discrimination of clay-based materials relies primarily on major element oxides (Cox et al., 1995; Roser and Korsch, 1988). As only major elements are considered, subtle compositional differences may remain undetected, resulting in a differentiation where samples might appear sometimes more similar than they are. Incorporating trace element data such as Ni, Cr, Rb, Zr, Y and Th/Sc and Cr/Th ratios could potentially provide a higher provenance resolution. Electron microprobe analysis (EPMA) would be a suitable approach to obtain such information (Freestone, 1982). Moreover, rare earth elements and associated REE profiles offer additional provenance potential, as they are not fractionated from each other by most sedimentary processes (Potter et al., 2005). Recently also, Sr and Pb isotope analyses proved to be effective to distinguish specific mudstone formations (Makarona et al., 2016).

To conclude, the SEM-EDS results further underscored the advantages of utilizing thin section petrography for classifying mudstone types, as it facilitated the identification of specific chemical trends and variability within the petrographic mudstone types. On a few occasions, the chemistry of the inclusions is not conclusive without petrographic structural information. In the case of mudstone 6, the established petrographic characteristics are pivotal as the chemical composition is rather in line with grog/clay-based material. As the influence of firing temperature on the mudstones is found to be minimal, demonstrated through tests conducted on reference mudstone of the Isfahan area, the mudstone types appear to be predominantly related to various outcrops. These findings not only elucidate the anticipated chemical signature of mudstones in the Kur River Basin but also show the intra-basin variability of mudstone and the potential of using thin section petrography with SEM-EDS as a robust tool for identifying and provenancing these frequently occurring materials in earthenwares.

## 5. Conclusions

This study reflects and builds on the criteria and methodology to differentiate grog and mudstone systematically and as reliably as possible in archaeological ceramics by using optical microscopy (thin section petrography) and scanning electron microscopy coupled with an energy dispersive spectrometer (SEM-EDS). We established and assessed a set of characteristic features using experimental testbars for distinguishing between mudstone and grog temper, demonstrating that mudstones typically exhibit high compactness, fine-grained textures, a high homogeneity, internal polygonal cracking patterns, higher roundness, a higher likelihood of birefringence in unsintered matrices, and can expose more variation in size range. Differentiation becomes increasingly more complicated when sintering occurs at higher firing temperatures, especially when fine grog is used. In such cases, the main remaining petrographic criterion is the roundness. Our findings highlight the variability and challenges inherent in accurately identifying mudstones and the necessity of comprehensive analyses and a (experimental) reference framework that uses or tests these criteria and takes into account other information regarding the composition, hardness and firing temperature.

The combined use of optical microscopy and SEM-EDS analysis demonstrates that mudstone types can be effectively distinguished and substantiated through their chemical composition, which largely differs from that of grog materials, supporting the revised petrographic criteria used for classification. Moreover, SEM-EDS analysis reveals the local/regional geochemical signatures of mudstones within the Kur River Basin, showing the compositional variability that can be attributed to the Kur River Basin in general and how these differ from other mudstone types further afield. Since mudstone chemistry can vary between outcrops, integrating this variability with a mudstone typology through thin section petrography can offer a solid provenancing and characterization approach, especially in sedimentary contexts.

## CRediT authorship contribution statement

**Possum Pincé:** Writing – review & editing, Writing – original draft, Visualization, Validation, Supervision, Software, Resources, Project administration, Methodology, Investigation, Funding acquisition, Formal analysis, Data curation, Conceptualization. **Negar Abdali:** Data curation. **Dennis Braekmans:** Writing – review & editing, Writing – original draft, Visualization, Validation, Supervision, Software, Resources, Project administration, Methodology, Investigation, Funding acquisition, Formal analysis, Data curation, Conceptualization.

## Declaration of competing interest

The authors declare that they have no known competing financial interests or personal relationships that could have appeared to influence the work reported in this paper.

## Acknowledgements

The authors express their gratitude to Prof. Dr. Holly Pittman and Katherine Blanchard of the Penn Museum (Philadelphia, USA) for granting access to their ceramic collections and allowing the subsampling of materials. We also sincerely thank Eric Mulder for his assistance in preparing the experimental batches at the Laboratory for Material Culture Studies, Leiden University. Furthermore, appreciation goes to Prof. Dr. Philippe Crombé, Prof. Dr. Johan De Grave and Prof. Dr. Stijn Dewaele for providing access to the optical and electronic microscope at the Geology Department of Ghent University. The SEM research was also generously supported by the Cranfield Forensic Institute, Cranfield University. The thin section experimental reference collection at Leiden was kindly supported by a Leiden University Fund/Bakels Fund project grant (www.luf.nl). Finally, we sincerely thank the reviewers for their constructive comments that helped strengthen the manuscript.

## Appendix A. Supplementary data

Supplementary data to this article can be found online at https://doi.org/10.1016/j.jas.2025.106419.

## Data availability

All data supporting the findings of this study are provided in the Supplementary Information files accompanying this article. Additional details or clarifications are available from the corresponding author upon reasonable request.

## References


Adams, A.E., MacKenzie, W.S., Guilford, C., 2015. Atlas of Sedimentary Rocks Under the Microscope. Routledge, London. https://doi.org/10.4324/9781315841243.

Alden, J.R., 1979. Regional Economic Organization in Banesh Period Iran. University of Michigan. Michigan.

Alden, J.R., Heskel, D., Hodges, R., Johnson, G.A., Kohl, P.L., Korfmann, M., Lamberg-Karlovsky, C.C., Le Brun, A., Vallat, F., Levin, L.D., Marchese, R.T., Mellaart, J., Nissen, H.J., Shaffer, J.G., Watkins, T., 1982. Trade and politics in proto-elamite Iran. Curr. Anthropol. 23 (6), 613–640.

Alden, J.R., Abdi, K., Azadi, A., Biglari, F., Heydari, S., 2004. Kushk-e hezar: a Mushki/Jari period site in the Kur River Basin. Fars, Iran. Iran 42, 25–45.

Alden, J.R., 2013. The Kur River Basin in the Proto-Elamite era. In: Ancient Iran and Its Neighbours - Local Developments and Long-Range Interactions in the Fourth Millennium BC, the British Institute of Persian Studies - Archaeological Monographs Series. Oxbow books, Oxford, pp. 207–232.

Alden, J.R., Petrie, C.A., 2015. New radiocarbon dates for the banesh period occupation at Tal-e Kureh. Fars, Iran. Iran LIII 185–189.

Arnold, D.E., 1985. Ceramic Theory and Cultural Process. Cambridge University Press, Cambridge.

Barley, N., 1994. Smashing Pots: Works of Clay from Africa. The British Museum Press, London, United Kingdom.

Blackman, J.M., 1981. The mineralogical and chemical analysis of Banesh period ceramics from Tal-e Malyan, Iran. In: Hughes, M.J. (Ed.), Scientific Studies in Ancient Ceramics. British Museum, London, pp. 7–20.

Blackman, J.M., 1988. Ceramic technology and problems of social evolution in Southwestern Iran: materials issues in art and archaeology. In: Proceedings from the Materials Research Society Symposium Reno, April 6-8 1988. Presented at the Materials Research Society, Pittsburgh, pp. 103–108.

Carter, E., Stolper, M.W., 1984. Elam: Surveys of Political History and Archaeology, near Eastern Studies. University of California Press, Berkeley and Los Angeles.

Cuomo di Caprio, N., Vaughan, S.J., 1993. Differentiating grog (Chamotte) from natural argillaceous inclusions in ceramic thin sections. Archeomaterials 7, 21–40.

Costin, C.L., 1991. Craft specialization: issues in defining, documenting, and explaining the Organization of Production. In: Schiffer, M.B. (Ed.), Archaeological Method and Theory 3. The University of Arizona Press, Tucson, pp. 1–56.

Cox, R., Lowe, D.R., Cullers, R.L., 1995. The influence of sediment recycling and basement composition of evolution of mudrock chemistry in the Southwestern United States. Geochem. Cosmochim. Acta 59, 2919–2940.

Cultrone, G., Rodriguez-Navarro, C., Sebastian, E., Cazalla, O., De La Torre, M.J., 2001. Carbonate and silicate phase reactions during ceramic firing. Eur. J. Mineral 13 (3), 621–634. https://doi.org/10.1127/0935-1221/2001/0013-0621.

Daszkiewicz, M., Maritan, L., 2016. Experimental firing and re-firing. In: Hunt, A. (Ed.), The Oxford Handbook of Archaeological Ceramic Analysis. Oxford University Press, Oxford, pp. 487–514.

Emami, M., Chapoulie, R., Abdi, K., 2021. Cathodoluminescence microscopy for interpreting the fabric and heating process of ancient pottery: Preliminary study on the technological features of pottery from the Kur River Basin. Archaeometry 64, 337–356.

Eramo, G., 2020. Ceramic technology: how to recognize clay processing. Archaeol. Anthropol. Sci. 12, 164. https://doi.org/10.1007/s12520-020-01132-z.

Fabbri, B., Gualtieri, S., Shoval, S., 2014. The presence of calcite in archeological ceramics. J. Eur. Ceram. Soc. 34, 1899–1911. https://doi.org/10.1016/j.jeurceramsoc.2014.01.007.

Freestone, I.C., 1982. Applications and potential of electron probe micro-analysis in technological and provenance investigations of ancient ceramics. Archaeometry 24, 99–116.

Gliozzo, E., 2020. Ceramic technology. How to reconstruct the firing process. Archaeological and Anthropoogical Sciences 12, 260. https://doi.org/10.1007/s12520-020-01133-y.

Gosselain, O.P., 1999. In pots we trust. The processing of clay and symbols in Sub-Saharan Africa. J. Mater. Cult. 4, 205–230.

Gosselain, O., Livingstone-Smith, A., 2005. The source clay selection and processing practices in Sub-Saharan Africa. In: Livingstone-Smith, A., Bosquet, D., Martineau, R. (Eds.), Pottery Manufacturing Processes: Reconstruction and Interpretation. BAR International Series, Oxford, pp. 33–47.

Gosselain, O., 2008. Thoughts and adjustments in the potter's backyard. Breaking the Mould: challenging the past through pottery. Prehistoric Ceramics Research Group: Occas. Pap. 6, 67–79.

Heimann, R.B., Maggetti, M., 2014. Ancient and Historical Ceramics: Materials, Technology, Art and Culinary Traditions. Schweizerbart Science Publishers, Stuttgart.

Holmqvist, E., Larsson, Å.M., Kriiska, A., Palonen, V., Pesonen, P., Mizohata, K., Kouki, P., Räisänen, J., 2018. Tracing grog and pots to reveal Neolithic corded ware culture contacts in the Baltic Sea region (SEM-EDS, PIXE). J. Archaeol. Sci. 91, 77–91. https://doi.org/10.1016/j.jas.2017.12.009.

Holmqvist, E., 2021. Why not let them rest in pieces? Grog-Temper, its provenance and social meanings of recycled ceramics in the Baltic Sea Region (2900–2300 BCE). Archaeometry 64, 8–25.

Kreiter, A., Kalicz, N., Kovacs, K., Siklosi, Z., Orsolya, V., 2017. Entangled traditions: lengyel and Tisza ceramic technology in a late Neolithic settelement in northern Hungary. J. Archaeol. Sci.: Report 16, 589–603.

Lazar, O.R., Bohacs, K.M., Macquaker, J.H.S., Schieber, J., Demko, T.M., 2015. Capturing key attributes of fine-grained sedimentary rocks in outcrops, cores, and thin Sections: nomenclature and description guidelines. J. Sediment. Res. 85, 230–246. https://doi.org/10.2110/jsr.2015.11.

Makarona, C., Mattielli, N., Laha, P., Terryn, H., Nys, K., Claeys, P., 2016. Leave no mudstone unturned: geochemical proxies for provenancing mudstone temper sources in South-Western Cyprus. J. Archaeol. Sci.: Report 7, 458–464. https://doi.org/10.1016/j.jasrep.2015.08.012.

Maniatis, Y., Tite, M.S., 1978. Ceramic technology in the Aegean world during the Bronze Age. In: Doumas, C. (Ed.), Thera and the Aegean World. Papers Presented at the Second International Scientific Congress, Santorini, Greece, August 1978, pp. 483–492. London.

Mason, R., Cooper, L., 1999. Grog, Petrology, and Early Transcaucasians at Godin Tepe, vol. 37, pp. 25–31. Iran.

Matson, F.R., 1972. Ceramic studies. In: McDonald, W.A., Rapp, Jr. G.R. (Eds.), The Minnesota Messenia Expedition. University of Minnesota, North Central Publishing Company, St. Paul, pp. 200–224.

Norris, D., Braekmans, D., Shortland, A., 2022. Technological connections in the development of 18th and 19th century Chinese painted enamels. J. Archaeol. Sci.: Report 42, 103406. https://doi.org/10.1016/j.jasrep.2022.103406.

Öhlinger, B., Tenconi, M., Maritan, L., Montana, G., Roppa, A., 2023. Technological choices and practices in local ceramic production at Iron Age Monte Iato (Sicily, 6th-5th century BCE). J. Archaeol. Sci.: Report 52, 104283.

Pincé, P., 2018. Clay in Close-Up: a Spectroscopic and Petrographic Approach to Ceramic Production in the Kur River Basin (Fars, Iran). Ghent University, Ghent.

Pincé, P., Braekmans, D., Abdali, N., Pauw, E.D., Amelirad, S., Vandenabeele, P., 2018. Development of ceramic production in the Kur River Basin (Fars, Iran) during the Neolithic: a compositional and technological approach using X-Ray fluorescence spectroscopy and thin section petrography. Archaeol. Anthropol. Sci. 11, 1241–1258. https://doi.org/10.1007/s12520-018-0598-6.

Pincé, P., Braekmans, D., Lycke, S., Vandenabeele, P., 2019. Ceramic production in the Kur River Basin (Fars, Iran) during the middle to late second millennium BCE: a geochemical and technological characterization. Archaeometry 61, 556–573. https://doi.org/10.1111/arcm.12451.

Potter, P.E., Maynard, J.B., Depetris, P.J., 2005. Mud and Mudstones. Springer, Berling-Heidelberg.

Quinn, P.S., 2013. Ceramic petrography: the interpretation of archaeological pottery & related artefacts in thin section. Archaeopress. Oxford.

Quinn, P.S., 2022. Thin section petrography, geochemistry and scanning Electron microscopy of archaeological ceramics. Archaeopress. Oxford.

Reed, S.J.B., 2005. Electron Microprobe Analysis and Scanning Electron Microscopy in Geology. Cambridge University Press, Cambridge.

Reedy, C.L., 2008. Thin-Section Petrography of Stone and Ceramic Cultural Materials. Archetype, London.

Rice, P.M., 1987. Pottery Analysis: a Sourcebook. University of Chicago Press, Chicago and London.

Roser, B.P., Korsch, R.J., 1988. Provenance signatures of sandstone mudstone suites determined using discriminant function analysis of major-element data. Chem. Geol. 67, 119–139.

Rye, O.S., 1981. Pottery Technology: Principles and Reconstruction. Taraxacum Inc., Washington.

Santacreu Albero, D., 2014. Materiality, Techniques and Society in Pottery Production: the Technological Study of Archaeological Ceramics Through Paste Analysis. De Gruyter, Warsaw/Berlin.

Sumner, W.M., 1972. Cultural Development in the Kur River Basin, Iran: an Archaeological Analysis of Settlement Patterns. University of Pennsylvania, Michigan.

Sumner, W.M., 1991. Ceramics vi. Uruk, proto-elamite, and early Bronze Age in Southern Persia. In: Encyclopaedia Iranica, pp. 284–288.

Sumner, W.M., 2003. Early urban life in the land of anshan: excavations at Tal-e Malyan in the highlands of Iran (no. 219). Malyan Excavation Reports. University of Pennsylvania, Philadelphia.

Taylor, S.R., McLennan, S.M., 1985. The Continental Crust: Its Composition and Evolution. Blackwell Scientific, Oxford.

Thér, R., 2014. Identification of pottery firing structures using the thermal characteristics of firing: identification of pottery firing structures using thermal characteristics. Archaeometry 56, 78–99. https://doi.org/10.1111/arcm.12052.

Tite, M.S., Freestone, I.C., Meeks, N.D., Bimson, M., 1982. The use of scanning electron microscopy in the technological examination of ancient ceramics. In: Olin, J., Franklin, A.D. (Eds.), Archaeological Ceramics. Smithsonian University Press, Washington D.C.

Tite, M.S., 1995. Firing temperature determinations - how and why? In: Lindahl, A., Stilborg, O. (Eds.), The Aim of Laboratory Analyses of Ceramics in Archaeology, Konferenser. Kungl. Vitterhets och Antikvitets Akademien, Lund, pp. 37–42.

Wang, S., Gainey, L., Mackinnon, I.D., Allen, C.M., Gu, Y., Xi, Y., 2023. Thermal behaviors of clay minerals as key components and additives for fired brick properties: a review. J. Build. Eng. 66, 105802. https://doi.org/10.1016/j.jobe.2022.105802.

Whitbread, I.K., 1986. The characterisation of argillaceous inclusions in ceramic thin sections. Archaeometry 28, 79–88.

Whitbread, I.K., 1995. Appendix 3: the collection, processing and interpretation of petrographic data. In: Greek Transport Amphorae: a Petrographical and Archaeological Study. British School at Athens, London, pp. 365–395.